TORQUE RIPPLE AND RADIAL FORCE REDUTION OF SRM WITH ROTOR POLE DESIGN

[1]Minh Dinh Bui, [2]Dinh Hai Linh and [3]Dang Chi Dung
Electrical Engineering Department
School of Electrical Engineering, Hanoi Unviversity of Science and Technology
Email: dinh.buiminh@hust.edu.vn

ABSTRACT

The stator and rotor pole structure and power inverters have significant influence on electromagnetic torque performances and efficiency performances. Many papers have investigated on those design parameters on motor result. Inductance and flux linkage will be influenced by rotor and stator pole combination and magnetic circuit. In this paper, a SRM 24/16 rotor shoe will improved form conventional SRM with the same outer diameter stator and stack length. The paper will investigate some rotor pole topologies to get reduce harmonic torque ripple. Radial forces of SRM 24/16 with normal and shoe pole have been compared and the shoe pole structure has more advantages.

Key words: *Switched Reluctance Motor - SRM, Pole Shoe, Torque ripples, Finite element Method - FEM.*

1. Introduction

Nowadays, Switched Reluctance Motor (SRM) has been chosen as the right candidate to drive this small scale electric vehicle due to the advantages of simple construction, wide constant power region and effective torque speed characteristic. SRMs have been applied in various fields, from automotive vehicles to the aircraft engine areas. However, power density and torque density are not as high as permanent magnet motors. The torque and efficiency performance can be improved by electromagnetic design and power inverter control method. In SRM, the number of stators, rotor and winding phase must be followed a regular. The number of phases m is calculated with the number of stator poles N_s and rotor poles N_r: [11]

$$m = \frac{N_s}{|N_s - N_r|} \qquad (1)$$

The cross-section of a three-phase SRM 6/4 with one phase of its associated power converter. Each phase of the machine is made up of two coils wound around diametrically opposed stator poles and electrically connected in series. In the SRM, torque is produced by the tendency of the nearest rotor poles to move to a minimum reluctance position with respect to the excited stator pole pair.

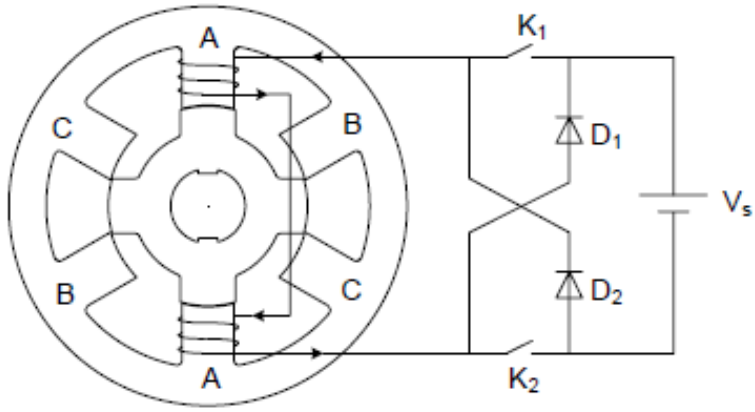

Figure 1. Three –phase SRM geometry and power converter topology

The pole arcs of the stator and rotor are important variables in the switched reluctance machine design as figure 1. In this paper, a three phase 6/4 SRM, the stator and rotor pole arcs are varied for a given current, and their effect on the average torque developed in the machine is studied to give a clearly identifiable range of practical pole arcs for rotor poles.

2. Electromagnetic Magnetic Torque

Number of stator poles Ns and the number of rotor poles Nr are determined by special applications and power converter topology. There are many possible combinations for the number of poles for SRM 6/4;12/8 and 24/16. The advantages and disadvantages have been explored in detail in[13]. This paper focuses on the popular combination of 24 stator poles and 16 rotor poles to improve torque performances in wide ranger speed.

The stator and rotor pole angle selection form a crucial part of the design process. There are many guidelines to be followed during the selection process. The standard design normally has the stator pole arc angle βs smaller than the rotor pole angle βr. The constraints on the values of pole arc angles are as follows: Rotor pole arc (β_r) is selected to be equal or greater than stator pole arc (β_s), since the number of rotor pole is less than number of stator pole ($\beta_s \leq \beta_r$). βs should be equal or greater than step angle to generate required torque. When βs is selected as smaller than step angle ($\beta_s < \varepsilon$), none of the phases may not have rising inductance slope, there may be some positions in the machine from where the machine may not start[13]. Step angle is shown by

$$\varepsilon = \frac{4\pi}{N_s.N_r} \tag{2}$$

Where ε is step angle.

Rotor pole angle should be greater than sum of stator and rotor pole arc as follows:

$$\beta_r \geq \beta_s\,;\ \beta_r + \beta_s < \frac{2\pi}{N_r}\,;\ \min(\beta_r, \beta_s) \geq \frac{2\pi}{m.N_r} \tag{3}$$

There are three constraints in determining the poles arc angle. These constraints are shown in the form of a triangle named Feasible Triangle. According to these restrictions, the ranges can be specified as 15° ≤ βs, βs+βr < 45°, and 15° ≤ βr ≤ 30° for SRM 12/8. Pole embrace of SRM is an important factor to have a good performance of the motor. Therefore, it should be considered in the motor design. Pole embrace is defined as the ratio of pole arc to pole pitch. Embrace coefficient of SRM generally affects the rotor and stator tooth widths. It also influences the torque ripple and average torque. Hence, the selection of pole embrace has a significant importance for the performance of SRM.

To predict the performance characteristics of the SRM the knowledge about the relationship ψ(i,θ) is required. Flux-linkage of SRM depends on the current and rotor position. Flux linkage is related to the inductance and current in the electromagnetic circuit of a SRM phase and expressed by:

$$\Psi_k = \Psi(\theta, i_k) = L_k(\theta, i_k).i_k \tag{4}$$

Where L_k is the inductance of k phase. Just as literatures mentioned, L_k (θ, i_k) can be fit by:

$$L(\theta, i_k) = L_o(i_k) + L_1(i_k).\cos(N_r\theta + \pi) \tag{5}$$

And
$$L_o(i_k) = L(i_k).\cos(N_r\theta + \pi)\,; \tag{6}$$

Where:

$$L_o(i_k) = \frac{L_{k\max}(i_k) + L_{k\min}(i_k)}{2}; L_1(i_k) = \frac{L_{k\max}(i_k) - L_{k\min}(i_k)}{2}$$
$$L_{k\min} = L_u; \quad L_{k\max} = \sum_{n=0}^{3} a_n i_k^n \tag{7}$$

Lkmin(ik) is the unaligned position inductance and is assumed to be a constant. The phase torque is given as literature (3,4,5,6,7) derived:

$$T_k = \frac{-N_r.i_k^2}{4}\left[\left(\sum_{n=0}^{3}\frac{2a_n}{n+2}i_k^n - L_{k\min}(i_k)\right)\sin(N_r\theta)\right] \tag{8}$$

Result of model the complete inductace profile and flux linkage are show in Figure 2,3.

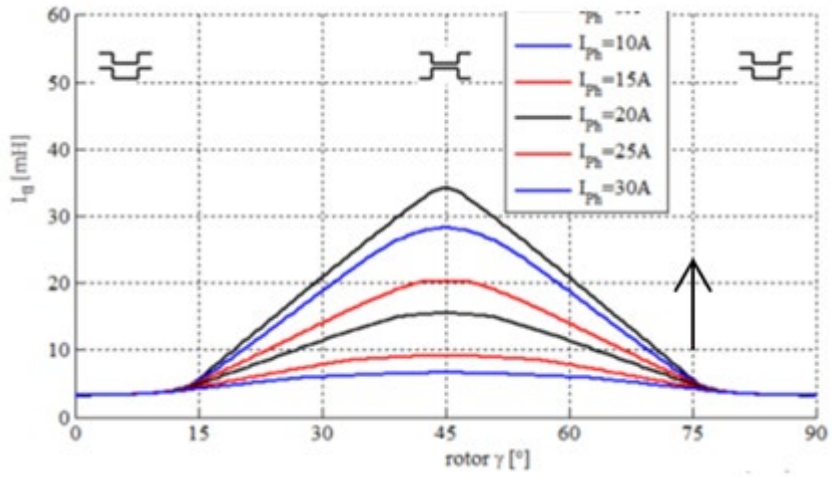

Figure 2. Inductance vs rotor position

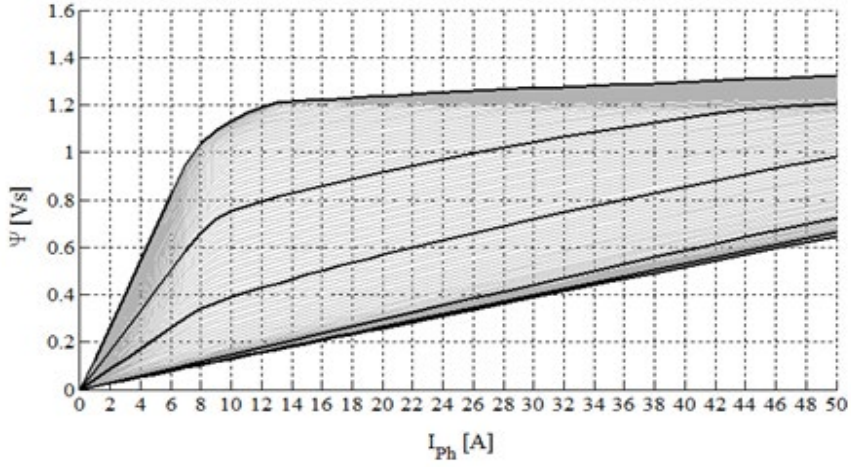

Figure 3. Flux linkage vs current with various rotor positions

From the flux linkage and inductance results in Figure 2&3 , a dynamic simulation has built to evaluate average torque, efficiency, and torque ripple performances.

3. Analytical Calculation and FEM Simulation Program

Since FEMM was first introduced, this program has been spread widely due to several reasons, particularly due to opensource code and free license. Unlike other finite element analysis program, FEMM allows the user can edit its code by themselves, to optimize and improve the calculation accuracy and speed in each problem. By coupling with Matlab, it has a strong calculation ability with easy to use in structure and programming. Furthermore, the design model in Simulink automatically with using several circuit topologies is also considered in future work. The program was developed for the purpose of combining all design process into one program. It allows to exchange the data between design process and simulation process. This is done by monitoring and active collecting results from both process when they were executed.

Design program is developed in Matlab environment. The analytical calculation can be used and stored by MATLAB programming language; the program interface was developed by Matlab GUI. After calculation, the system can present on screen as well as export drawings in dxf type. All drawings can be development works involve the integrated environment linking analytical calculation to simulation environment of FEMM.

This program has functions of sizing, overlapped the rotor slot, changing the size and worse performance report. The program must find the best choice for both, using regression. Collecting and responding data concept is also quite simple. There are only some special parameters of the motor to be verified, for example, output torque or the air gap flux density. The output torque is taken by a block integral of the shaft and the air gap flux density similarly can be collected by function. All result will be stored in database and used for further comparison. In addition, results which belonged to calculation progress and resulted in simulation progress are saved separately in 2 files. The program is divided into three main parts: analytical calculation, exporting drawing and magnetic simulation as Figure 4. There are also some supporting parts including material library which also associate with FEMM library.

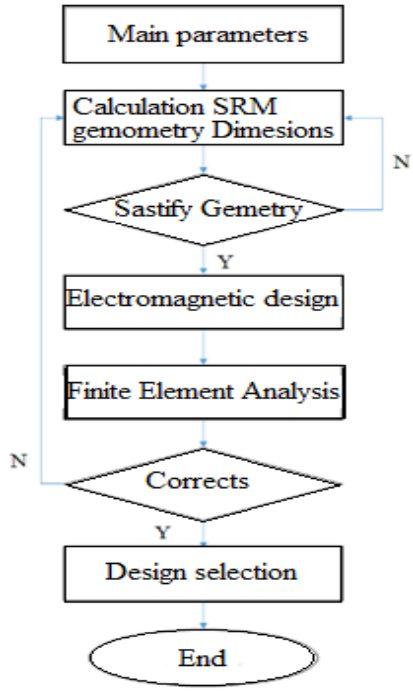

Figure 4. Program Structure

The program interface is well defined set of Matlab function to parse, manage and interpole data. There are some parameters which was provided in the program, but only some important results will be displayed and to be divided into tabs. The interface is written by Matlab GUIDE. There is menu, button, and pop-up menu to manipulate, main parameters and material library must be selected first. The calculation progress is not activated without these parameters, e.g, power, torque, pole numbers…, however, there are default materials for each part of the motor. The interface links to database, material library as well as calculation results. When the system receives main parameters for motors, calculations will be executed. The results will be stored in database in file.mat format. Electrical steel material will be defined by specific parameters. The wire library includes the diameter, electrical conductivity. Electrical steel parameters consist of B-H curve and electrical conductivity. In motor core materials of industrial applications, low iron loss is required for high motor efficiency [3-8], and high magnetic flux density is required for motor downsizing and high torque. To reduce the iron loss of electrical steel sheets, Si addition is effective from the viewpoints of increasing resistivity and decreasing magnetic anisotropy, and approximately 3% Si is added to high grade electrical steel sheets as figure 5.

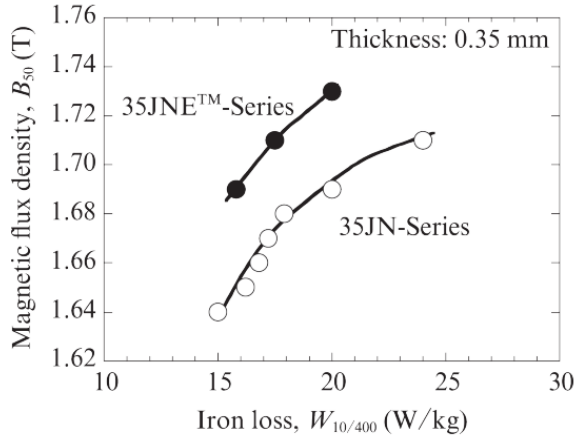

Figure 5. Silicon steel B-Ironloss curves

Following main parameters and material library, there will be analytical analysis. The analyzing process will be started by choosing motor length, diameter and height based on motor standard. During the process, there are some experience coefficients which were defined before. All dimensions of motor will be calculated, including stator slot, rotor slot, airgap. This process is same as induction motor design. In details, stator slot size is calculated mainly based on stator winding which depended on power, current and experience coefficients. After analytical results are achieved, all the dimensions of motor are saved in database in matrix form. When the export command is generated, the drawing process will be executed. The program was developed by MATLAB DXF library. Unfortunately, the library is quite simple, all difficult tasks, such as drawing circle line, rotating object, are achieved by geometrical formulas. To do this, circle line is made from several line, to draw a line, start point and end point are required. Using minimum number of lines will help the system to store a lot of data, which will result slowing down speed and difficulties when exporting the drawings to another software. In the other hand, rotating and mirror is also a difficult task in programming. The strategy, using loop function to redraw several times and using trigonometric function with angle steps, is applied and returns good results. The system will export 3 drawings: motor, rotor, and stator separately. These drawings can be used in several simulation program and design and manufacturing progress.

4. SRM 24/16 Rotor Pole Comparison

In this study, a SRM 24/16 1.2 kW- 1500rpm are carried out and the Electromagnetic analyses are performed for the reference motor and then two different SRM rotor designs are realized. The SRM

24/16 with different rotor shapes are investigated in detail using FEA and several parametric optimizations are also performed before finalizing the design.

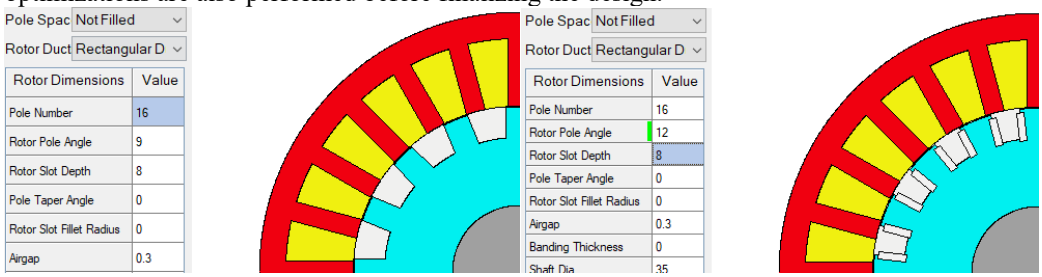

Figure 6. SRM 24/16 with normal pole (a) and shoe pole (b)

The shoe pole has bigger surface area or larger rotor embrace which can keep higher flux density in airgap. The geometry parameters of the SRM 24/16 were listed in Table1.

Table 1. Geometry parameters of SRM 24/16

Parameter	Unit	SRM 12/8
Stator Poles		24
Stator Pole Angle	degree	7
Stator Lam Dia	mm	140
Stator Bore	mm	90
Stator Pole Depth	mm	15
Pole Number		16
Rotor Pole Angle	degree	16
Rotor Slot Depth	mm	11
Airgap	mm	0.3

The FEA program has been calculated with two rotor pole shapes and the rotor pole shoe has better average torque and efficiency.

Table 2. Torque and Efficiency Comparison of SRM 24/16

Parameters	Shoe pole	Normal pole	Unit
Average torque	10.899	9.6484	Nm
Torque Ripple	6.5973	6.9156	Nm
Torque Ripple [%]	61.701	72.622	%
Electromagnetic Power	1679.5	1495.8	Watts
Input Power	1928.4	1726.5	Watts
Output Power	1636.5	1460.5	Watts
Total Losses (on load)	291.86	266.01	Watts
System Efficiency	84.865	84.593	%
Shaft Torque	10.418	9.2978	Nm

Electromagnetic torque waveforms of the SRM 24/16 with normal and shoe poles were plotted in Figure 7. The torque ripple of SRM shoe pole is smaller than the normal poles. To verify torque ripple performances, harmonic torque orders can be analyzed in follow steps.

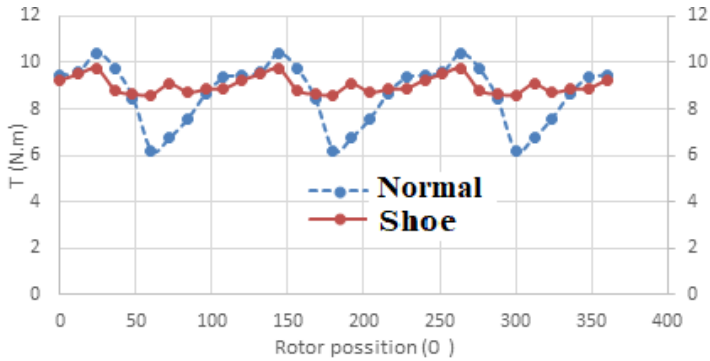

Figure 7. SRM 24/16 with normal pole and shoe pole torque curves

Torque harmonics are generated due to the different phase torque interaction, and they can be reduced by applying rotor pole angle and shape designs. The total torque is combined by harmonic the harmonic torques which depend on flux density and current waveform. Then, its effectiveness is clarified according to the representative control strategies for induction motor such as maximum torque per ampere and flux-weakening control.

The electromagnetic torque can be expressed by a series of harmonics

$$T_e = T_0 + \sum_{n=1}^{N} T_n \cos(\mathrm{n}\theta + \varphi_n) \qquad (9)$$

with $T_n = \frac{N_r}{2\pi} \int_0^{2\pi/N_r} T_e(\theta)\cos(n.N_r.\theta + \varphi_n)d\theta$

The electromagnetic torque, torque ripple and efficiency of SRM 24/16 has been evaluated in figure 8, and the performances of SRM rotor with shoe pole is better than the rotor normal poles.

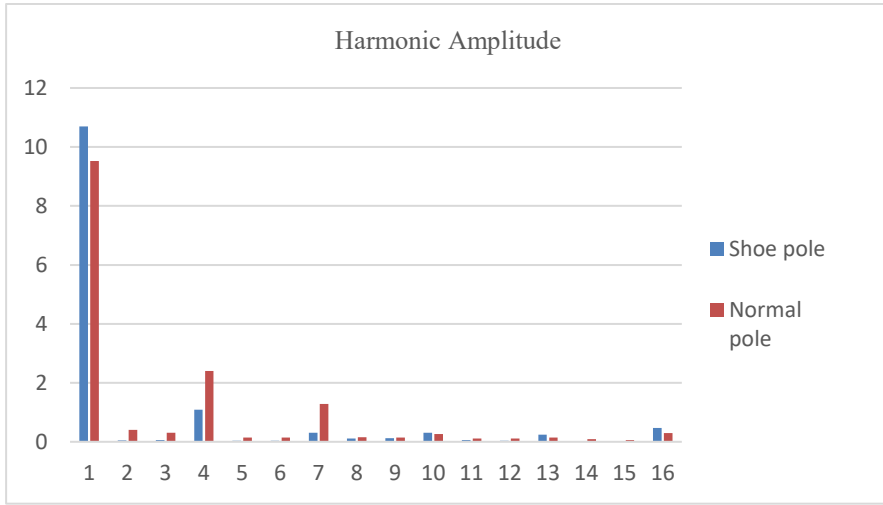

Figure 8. Harmonic torque with normal pole (a) and shoe pole (b)

The tangential force density and radial force density in the air gap are given by:

$$f_t = \frac{1}{2\mu_0} 2B_r B_t$$

$$f_r = \frac{1}{2\mu_0}(B_r^2 - B_t^2)$$

where f_t and f_r are the tangential and radial force densities respectively; B_t and B_r are the tangential and radial magnetic flux intensities from the tangential and vertical directions, respectively.

Electromagnetic force has been calculated by analytical model, the radial and tangential forces were plotted in figure 9

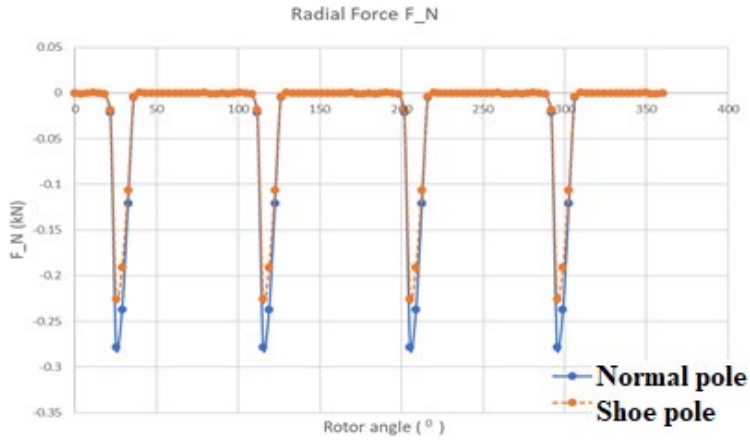

Figure 9. Radial forces with normal pole (a) and shoe pole (b)

Radial force value (0.22 kN) with shoe pole is smaller than normal pole (0.28kN) because the air gap flux density is evenly.

5. CONCLUSION

The article has analyzed rotor pole design influenced on average torque and torque ripples by FEM simulation method. The average torque, torque ripple and efficiency have been compared in between normal rotor and shoe pole. The shoe hole structure has higher efficiency and lower torque ripple. The stator and rotor geometry parameters were kept the same and phase winding and turn per coil were fixed. This paper has also presented a novel rotor structure to reduce electromagnetic force. The shoe pole contributes to change the flux path and flatten flux density in air gap that radial force can be reduced while maintaining the average torque. Finite element analysis was performed to verify the radial and tangential force. The result shows that the radial force can be improved, and the average torque is even slightly higher than the conventional structure.

REFERENCES

1. M. A. Raj and A. Kavitha, “Effect of Rotor Geometry on Peak and Average Torque of External-Rotor Synchronous Reluctance Motor in Comparison With Switched Reluctance Motor for Low-Speed Direct-Drive Domestic Application,” *IEEE Transactions on Magnetics*, vol. 53, no. 11, pp. 1–9, 2017, doi: 10.1109/TMAG.2017.2710191.
2. J. Han, B. Ge, K. Zhang, Y. Wang, and C. Wang, “Influence of control and structure parameters on the starting performance of a 12/8 pole switched reluctance motor,” *Energies*, vol. 13, no. 14, 2020, doi: 10.3390/en13143744.
3. N. K. Sheth and K. R. Rajagopal, “Optimum Pole Arcs for a Switched Reluctance Motor

for Higher Torque with Reduced Ripple," *IEEE Transactions on Magnetics*, vol. 39, no. 5 II, pp. 3214–3216, 2003, doi: 10.1109/TMAG.2003.816151.
4. M. Yildirim and H. Kurum, "Influence of Poles Embrace on In-Wheel Switched Reluctance Motor Design," *Proceedings - 2018 IEEE 18th International Conference on Power Electronics and Motion Control, PEMC 2018*, pp. 562–567, 2018, doi: 10.1109/EPEPEMC.2018.8521859.
5. A. Tap, L. Xheladini, T. Asan, M. Imeryuz, M. Yilmaz, and L. T. Ergene, "Effects of the rotor design parameters on the torque production of a PMaSynRM for washing machine applications," *Proceedings - 2017 International Conference on Optimization of Electrical and Electronic Equipment, OPTIM 2017 and 2017 Intl Aegean Conference on Electrical Machines and Power Electronics, ACEMP 2017*, pp. 370–375, 2017, doi: 10.1109/OPTIM.2017.7974998.
6. A. Siadatan, M. Roohisankestani, and S. Farhangian, "Design and Simulation of a new Switched Reluctance Motor with changes in the shape of stator and rotor in order to reduce torque ripple and comparison with the conventional motor," *SPEEDAM 2018 - Proceedings: International Symposium on Power Electronics, Electrical Drives, Automation and Motion*, pp. 353–358, 2018, doi: 10.1109/SPEEDAM.2018.8445245.
7. V. Rallabandi, J. Wu, P. Zhou, D. G. Dorrell, and D. M. Ionel, "Optimal Design of a Switched Reluctance Motor with Magnetically Disconnected Rotor Modules Using a Design of Experiments Differential Evolution FEA-Based Method," *IEEE Transactions on Magnetics*, vol. 54, no. 11, pp. 1–5, 2018, doi: 10.1109/TMAG.2018.2850744.
8. A. Siadatan, N. Fatahi, and M. Sedaghat, "Optimum Designed Multilayer Switched Reluctance Motors for use in Electric Vehicles to Increase Efficiency," *SPEEDAM 2018 - Proceedings: International Symposium on Power Electronics, Electrical Drives, Automation and Motion*, pp. 304–308, 2018, doi: 10.1109/SPEEDAM.2018.8445215.
9. Z. Yueying, Y. Chuantian, Y. Yuan, W. Weiyan, and Z. Chengwen, "Design and optimisation of an In-wheel switched reluctance motor for electric vehicles," *IET Intelligent Transport Systems*, vol. 13, no. 1, pp. 175–182, 2019, doi: 10.1049/iet-its.2018.5097.
10. M. D. Bui, S. Schneider, S. Arnaout, and U. Schaefer, "Torque maximization of a high-speed switched reluctance starter in acceleration test," *2013 15th European Conference on Power Electronics and Applications, EPE 2013*, no. 1, pp. 1–5, 2013, doi: 10.1109/EPE.2013.6631908.
11. T. Wichert, "Design and construction modifications of switched reluctance machines," p. 161, 2008.
12. P. Vijayraghavan, "Design of Switched Reluctance Motors and Development of a Universal Controller for Switched Reluctance and Permanent Magnet Brushless DC Motor Drives Design of Switched Reluctance Motors and Development of a Universal Controller for Switched Reluctance an," *PhD Proposal*, 2001.
13. R. Krishnan, *Switched reluctance motor drives: Modeling, simulation, analysis, design, and applications*. 2017.

14. Biography

Minh Dinh Bui was born on Nov, 10th, 1978 in Hanoi/Vietnam and received the B.S. degree in electrical engineering from Hanoi University of Science and Technology, Vietnam, in 2003 and the M.Sc. degree in the Department of Electrical Engineering from Hanoi University of Science and Technology, Vietnam, in 2007. He has graduated doctor degree at Berlin Institute of Technology in April 2014. Currently, he is a teacher at Hanoi University of Science and Technology. He has some projects of design high speed Switched Reluctance Motor and High efficiency Line Start Permanent Magnet Motor

